Attenuation of random noise using advanced adaptive filters in post-stack seismic imaging

G. Brahmi[1], M.C. Berguig[1] and L. Harrouchi[2]

[1] Geophysics Laboratory and Geophysics Department, FSTGAT/USTHB, Algiers, Algeria

[2] Sahara Geology Laboratory, Kasdi Merbah University, Ouargla, Algeria

ABSTRACT   The main objective of this work is to propose a method based on adaptive filtering to reduce the random noise from post-stack seismic data. The random noise can be reduced from seismic data by stacking the traces in multiple coverage, filtering during processing or using arrays of geophones during data acquisition. Recently, several filters have been used in image processing to resolve or compensate the deficiencies of conventional filtering such as the Adaptive Median Filter and 2D Adaptive Wiener Filter. Therefore, Adaptive Median filtering has been applied widely in image processing as an advanced method compared to standard median filtering. In this study, we present a combination of the Adaptive Median Filter, 2D Adaptive Wiener Filter, and Adaptive Local Noise Reduction Filter applied to post-stacked synthetic and real seismic data. The different comparisons of resulting seismic sections and their power spectrum show that both the proposed methods of filtering improve seismic imaging of the faulted structures better than other used filters.

Key words: random noise, adaptive filtering, post-stack, power spectrum, similarity and signal to noise ratio.

1. Introduction

The seismic data processing sequence contains several types of filtering in order to reduce noise not attenuated by multiple coverage during acquisition (Telford *et al.,* 1990; Yilmaz, 2001). The filtering processing is applied to seismic data to attenuate the effect of noise and preserve the useful signal in order to produce a clean, high-resolution final seismic image. Thus, the main purpose of filtering operations is to obtain an interpretable seismic image, constituting a basic document for drilling. The seismic image is processed using appropriate techniques of signal processing and converted to digital forms and, thereafter, some operations are applied in order to obtain an enhanced image and extract some useful information (Gonzales and Woods, 2002).

Several methods of filtering have been proposed such as F-K filtering (Stewart and Schieck, 1993), median filtering (Bednar, 1983), Adaptive Noise Cancellation (Dragoset, 1995), F-x deconvolution (Canales, 1984), adaptive local thresholding by verification-based multithreshold probing with application to vessel detection in retinal images (Jiang and Mojon, 2003), curvelet thresholding (Neelamani *et al.,* 2008)**,** F-x empirical-mode decomposition predictive filtering (Chen and Ma, 2014), adaptive nonlocal means algorithm (Shang *et al.,* 2013), and T-x frequency filtering of high resolution seismic reflection data using singular spectral analysis (Rajesh *et al.,* 2014). The adaptive filtering constitutes an important tool in seismic data analysis with its

varieties such as the Lee filtering. Lee filtering is a standard deviation based (sigma) filter that operates on statistics by least squares estimation calculated within individual filter windows (Lee, 1980). The Frost filter is a circularly symmetric filter that uses local statistics (Zhenghao and Ko, 1994). The Kuan filter is similar to the Lee filter but uses a different weighting functional tested on deep seismic reflection data (Ristau and Moon, 2001).

Advanced adaptive filtering is considered an effective method to suppress speckle noise in 2D digital image data; a variety of adaptive filtering algorithms have been developed and employed to attenuate random noise from seismic data.

An adaptive noise attenuation method developed by Cai *et al*. (2014) for edge and amplitudes preservation involves decomposing the full-band seismic signal into multiband data and, then, processing using nonlinear anisotropic dip-oriented edge-preserving filtering. This method, based on high resolution processing, provides useful information for structural interpretation, specially to identify faults, breaking points, and horizon tracking. In the case of random noise, the useful signal is predicted by the autoregressive filter and the residual signal is assumed to be the noise (Bekara and Baan, 2009).

Moreover, Sacchi and Naghizadeh (2009) proposed an adaptive linear prediction filtering algorithm implemented via filters that are estimated from the inversion of a system of equations in the T-x or f-x domain for removing random noise in seismic imaging. Deng *et al.* (2015) propose an adaptive version of time-frequency peak filtering to remove random noise in seismic imaging.

Various algorithms of adaptive filters such as the Adaptive Median (AM) filter and 2D adaptive filter were widely used to denoise seismic sections. The two adaptive filters: optimum 2D median filter and 2D Adaptive Wiener (2DAW) filter were applied in 2D ultra-shallow seismic reflection and ground-penetrating radar data to suppress random noise (Jeng *et al.,* 2009). Gan *et al*. (2016) propose a structural-oriented median filter to attenuate the blending noise along the structural direction of seismic profiles, to flatten the seismic record in local spatial windows and, then, to apply a traditional Median Filter (MF) to the third flattened dimension and the estimation of the local slope, calculated by first scanning the Normal Moveout (NMO) velocity.

To reduce the noise, an efficient deblending framework using median filtering without requiring a correct NMO algorithm has also been proposed by Bai and Wu (2017): they propose an efficient based modified median filtering approach that does not require a correct NMO correction. Liu *et al.* (2019) propose an optimal adaptive bi-stable array stochastic resonance based grey-scale image restoration enhancement method under low peak signal-to-noise ratio environments. In this method, the Hilbert scanning is adopted to reduce the dimension of the original grey-scale image. Results show that the proposed method significantly outperforms the classical image restoration methods. As another efficient method, Chen *et al.* (2020) propose a type of structure-oriented median filter that can effectively attenuate spike-like noise, in which a structure-oriented space-varying median filter can adaptively squeeze and stretch the window length of the median filter. This method is applied to remove the spike-like blending noise arising from the simultaneous source acquisition. More recently, a new approach has been proposed by Saad and Chen (2020) to attenuate random noise based on a Deep-Denoising Auto-Encoder (DDAE) that encodes the input seismic data to multiple levels of abstraction, and, then, decodes those levels to reconstruct the filtered seismic signal.

In this work, we introduce some image-based filters, namely AM filter, 2DAW filter, and Adaptive Local Noise Reduction (ALNR) filter, to remove random noise from seismic stacked data. These methods are based on the estimation of the statistical parameters of the noise and signal, such as the mean and variance. We begin by briefly discussing the classic adaptive filtering based on the least mean squares (LMS) algorithm and its limitation.

We review the theory of some used filters, in particular the 2DAW filter, AM filter, and propose the new ALNR filter. Then, we apply the filter to synthetic and real stacked data to attenuate random noise, and compare different spectra of filtered images. As per image quality, these filters achieve a better result of edge preservation (reflections) and good quality for seismic imaging.

2. Review of adaptive filter based on LMS algorithm

There are two types of digital filters: fixed filter and adaptive filter. A fixed filter is useful when the parameters of signal and channel are known. On the other hand, adaptive filters are useful when the dynamics of the signal or channel is unpredictable and changes with time.

Adaptive filters are commonly used in image processing to enhance or restore data by removing noise without significantly blurring the structures in the image (Westin *et al.,* 2000). Adaptive filters have been popular since the early 1960s after they were studied and developed by Widrow (1959). His development is based on the theory of Wiener filters for optimum linear estimation. There are also other approaches to the development of adaptive filter algorithms, such as Kalman filters, least squares, etc (Sayed, 2003).

LMS is the most frequently used algorithm in adaptive filtering. It is basically a gradient descent algorithm, which means that it adjusts the adaptive filter coefficients by modifying them by an amount, which is proportional to the gradient of the error surface. This filter's algorithm is defined by the following system:

$$y(n) = W^T(n-1)u(n)$$
$$e(n) = d(n) - y(n)$$
$$W(n) = \alpha W(n-1) + f(u(n), e(n), \mu)$$

(1)

The LMS adaptive filter algorithms available in this system are defined as:

$$f(u(n), e(n), \mu) = \mu e(n)\mu * (n)$$

(2)

where *n is* the current time index, *u(n)* the vector of buffered input samples at step *n*, $\mu * (n)$ the complex conjugate of the vector of buffered input samples at step *n*, *W(n)* the vector of filter weight estimates at step *n*, *y(n)* the filtered output at step *n*, *e(n)* the estimation error at step *n*, *d(n)* the desired response at step *n*, μ the adaptation step size and α the leakage factor (0 < α ≤ 1). Fig. 1 shows an adaptive filter structure.

The LMS algorithm, as one of most popular adaptive algorithms for noise attenuation by adaptive filtering, has the advantage of easy implementation. LMS algorithms were tested in a MATLAB code; Fig. 2 shows the sinusoidal signal (in black) corrupted by 10% (magenta) and 50% (magenta) of random noise, in Figs. 2a and 2b, respectively. The results (in red) represents the signal filtered by an adaptive filter based on the LMS algorithm. However, the LMS algorithm has the disadvantage of serious signal distortion when the level of noise is high (Fig. 2b).
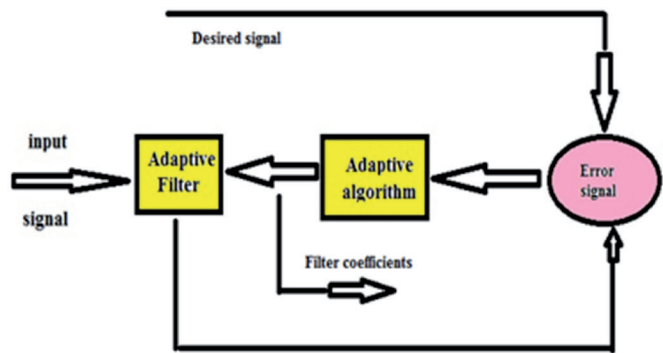
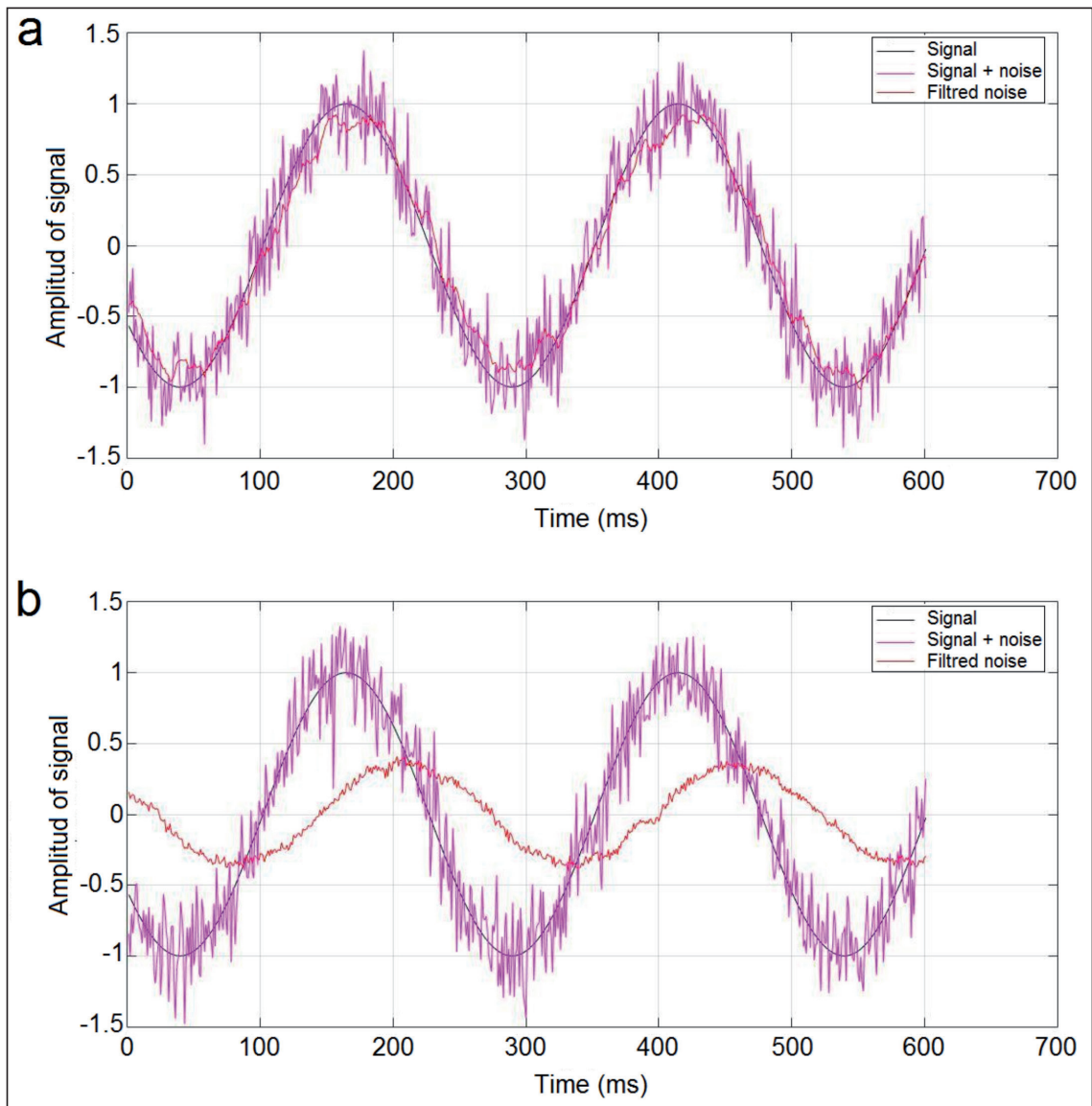Fig. 1 - Block diagram of an adaptive filter.

Fig. 2 - Example of a filtered sinusoidal signal by adaptive LMS filter after corrupting by 10% (a) and 50% (b) of random noise.

3. Proposed filters

3.1. The AM filter

Median filtering is a nonlinear method used to remove noise from images. The AM filter performs spatial processing to preserve detailed and smooth noise (Rakesh, 2018). It is very effective at removing noise while preserving edges. It is particularly effective in removing salt and pepper type noise. The median filter works by moving through the image pixel by pixel, replacing each value with the median value of neighbouring pixels. The pattern of neighbours is called the 'window', which slides, pixel by pixel, over the entire image. The median is calculated by first sorting all the pixel values from the window into numerical order, and, then, replacing the pixel being considered with the middle (median) pixel value. The median filter with variable window length is an AM filter, thus it can be conveniently used in the presented processing work or without the need for much human input (Bai and Wu, 2017).

The centre pixel of the window is evaluated to verify whether it is an impulse or not. If it is an impulse, then the new value of that pixel in the filtered image will be the median value of the pixels in that window. If, however, the centre pixel is not an impulse, then the value of the centre pixel is retained in the filtered image.

AM filtering can handle the filtering operation of an image corrupted with impulse noise of probability greater than 0.2. This filter also smoothens out other types of noise, thus, giving a much better output image than the standard median filter.

3.2. Implementation of algorithm

The AM filter works on a rectangular region S_{xy}. The AM filter changes the size of S_{xy} during the filtering operation depending on certain criteria as described below. The output of the filter is a single value which replaces the current pixel value at (x, y), the point on which S_{xy} is centred at the time. The following notation is reintroduced here:

Z_{min} = minimum grey level value in S_{xy},
Z_{max} = maximum grey level value in S_{xy},
Z_{med} = median of grey levels in S_{xy},
Z_{xy} = gray level at coordinates S_{xy},
S_{max} = maximum allowed size of S_{xy}.
The AM filter works in two levels, denoted Level A and Level B, as follows:
Level A: A1 = Z_{med} - Z_{min}, A2 = Z_{med} - Z_{max}.
If A1 > 0; and A2 < 0, go to level B, else increase the window size.
If window size ≤ S_{max} repeat level A,
else output Z_{xy}.
Level B: B1 = Z_{xy} - Z_{min}, B2 = Z_{xy} - Z_{max},
if B1 > 0, and B2 < 0 output Z_{xy}, else output Z_{med}.

3.3. The 2ADAW filter

The 2DAW filter is a real time optimal filter updated from the Wiener filter technology, which became available in 1940. A central problem in the application of random fields is the estimation of various statistical parameters from real data. The Wiener filter minimises the least squares error between the desired and actual outputs. The desired filter coefficients are

consequently obtained by solving a normal equation in matrix form, which is derived by a least squares error method. Subsequently, improved versions of the Wiener filter were introduced for image processing, for example a collaborative Adaptive Wiener Filter employs a finite size moving window for image restoration using a spatial-domain multi-patch correlation model (Mohamed and Hardie, 2015).

The classic Wiener filter can process a signal according to the variance within the entire time range but the shortfall is that it neglects the local characteristics of the signal. The Adaptive Wiener Filter can adjust the filtering output according to the local variance of the signal. When the local variance is large, the smoothing effect becomes strong. The result of the adaptive filter is better than that of a linear filter because it can protect edge and high frequency information of the signal (Liu *et al.,* 2006). Frequently the signals are corrupted by additive noise, so the measurement obtained, *y(n)*, is related to the original signal, *x(n)*, as follows:

$$y(n) = x(n) + v(n) \tag{3}$$

The Wiener filter is an optimal filter derived with respect to a certain objective criterion. Westin *et al*. (2000) describe how the Wiener filter may be designed to adapt to local and spatially variable details in images. The filter is cast as a combination of low-pass and high-pass filters, with factors that control their relative weights.

In the case of linear stationary estimation, we wish to estimate the process *f* with a linear combination of values of the data *g*. This can be expressed by a convolution operation: *f = h ∗ g*, where *h* is a linear filter. A very general statement of the estimation problem is: given a set of data *g*, find the estimate $\tilde{f}$ of an image *f* that minimises some distance: $||f - \tilde{f}||$ by local linear minimum mean squared error, also known as the Adaptive Wiener Filter; we can minimise the aforementioned distance under the following conditions.

Assume that the image is corrupted by additive noise. Minimise the local mean squared error by applying a linear operator to each pixel in the image. The local mean and variance are estimated from a rectangular window around the pixel. Lee (1980) derived an efficient implementation of a noise-adaptive Wiener filter by modelling the signal locally as a stationary process that results in the filter to estimate the original pixel value *f(m,n)* by the following relation (Bankman, 2009):

$$\tilde{f}(m,n) = \mu_g(m,n) + \left(g(m,n) - \mu_g(m,n)\right)\frac{\sigma_g^2(m,n) - \sigma_\eta^2(m,n)}{\sigma_g^2(m,n)} \tag{4}$$

where *g* is the corrupted image, μ_g is the local mean of signal *g*, σ_g^2 is the local variance and σ_η^2 is the variance of noise: it is constant if noise is signal-independent, it varies if noise is signal-dependent and in the latter case it should be estimated locally with the knowledge of the type of the noise.

3.4. The ALNR filter

ALNR filters were used to remove the watermark from the watermarked component in binary image, and the difference between the result and watermarked component is used to acquire an extracted watermark (Chotikawanid *et al.,* 2018).

ALNRF is based on the following formula:

$$h(i,j) = \begin{cases} f(i,j) - \dfrac{\sigma_n^2}{\sigma_L^2}\big[f(i,j) - \mu_L\big], if\, \sigma_n^2 \prec \sigma_l^2, \\ \mu_L \;\text{other wise} \end{cases}$$

(5)

where $h(i,j)$ is the new image, $f(i,j)$ the noisy image pixel value at position i and j, σ_n^2 noise variance, μ_L and σ_L^2, local mean and dispersion near pixel (i,j), we know that local mean (i,j):

$$\mu = \frac{1}{N^2} \sum_{i'=-N/2}^{N/2} \sum_{j'=-N/2}^{N/2} f(i+i', j+j')$$

(6)

and local variance (i,j):

$$\sigma^2 = \left(\frac{1}{N^2} \sum_{i'=-N/2}^{N/2} \sum_{j'=-N/2}^{N/2} f(i+i', j+j') \right)^2 - \mu^2$$

(7)

From Eq. 3, the behaviours of the filter can be characterised into 3 conditions:

if σ_n^2 is equal to zero, the result of the filter is a noisy image,

if σ_L^2 is much more than σ_n^2, $h(i,j)$ is equal to $f(i,j)$ to preserve edge information,

if σ_n^2 is equal to or greater than σ_L^2 the output of arithmetic mean filter in rectangular window size $m \times n$.

To improve the performance of the adaptive filter, a new algorithm has been developed that adds to the basic one the advantage of operating, when necessary, with a smaller window, near and in the presence of those small details that, by increasing the local variance, increases the ratio with the noise variance, beyond a certain threshold, supplied to the filter as an argument (https://github.com/infovillasimius/imadvfilter/blob/master/README.md).

Put simply, the basic function for thresholding creates the binary image from grey level ones by turning all pixels below some threshold to zero and all pixels above that threshold to one. If $g(i,j)$ is a threshold version of $f(i,j)$ at some global threshold T, g is equal to 1 if $f(x,y) \geq T$ and zero otherwise. Thus, the new image obtained by thresholding is expressed by the following law:

$$g(x,y) = \begin{cases} 0 \;\text{ if } f(x,y) \prec T \\ 1\,\text{if } f(x,y) \geq T \end{cases}$$

(8)

where T is calculated by Eq. 5.

If the ratio between the variances exceeds this threshold, the algorithm tries to check whether by decreasing the filter size, for that point, the ratio drops back below the threshold and, in this case, applies the basic formula. Otherwise the filter dimensions will continue to decrease until the minimum size (3×3) is reached. It, then, proceeds to check the value of the ratio of the variances and, if it is greater than 1, always applies the basic formula, replacing, otherwise, the value of the current pixel with the average of the 3×3 around it.

4. Application of the techniques to synthetic seismic images

Synthetic Trace is useful for creating model input data for any filter testing. We first tested the 2DAW filter, AM filter, and the ALNR filter on the synthetic seismic image. In order to test the applicability of our filters, from a geological model composed of three slightly inclined layers (Fig. 3), we generate a mini seismic section composed of 48 traces, the intertraces distance is 25 m. The synthetic seismogram is obtained by the convolution of Klauder synthetic wavelet with seismic reflection coefficients. We note that Klauder wavelet is the autocorrelation of a vibroseis sweep and has the same spectrum as a vibroseis sweep of any given length and frequency range. In our case the length of vibroseis sweep is 5000 ms and the frequency range is 12-72 Hz. It is worth noting that we were aware of the fact that the geological model attenuates the high frequencies when increasing in depth. By adding 25% of random noise to the synthetic model, this operation gives traces which have both data and noise for filters testing (Fig. 4a).

In order to test the efficiency of the filters to attenuate random noise, different windows are tested (3×3, 5×5, 7×7, 9×9, and 11×11 pixels) in a 2DAW filter (Fig. 4b), ALNR filters (Fig. 4c), and an AM filter (Fig. 4d). As shown, the difference between the original and filtered image is clear with inhomogeneous brightness and contrast. The root mean square (RMS) indicates the level of enhancement in the processed image (Fig. 4e). We found that for any filter, for the given values of the window it gives an empirically good denoised image.
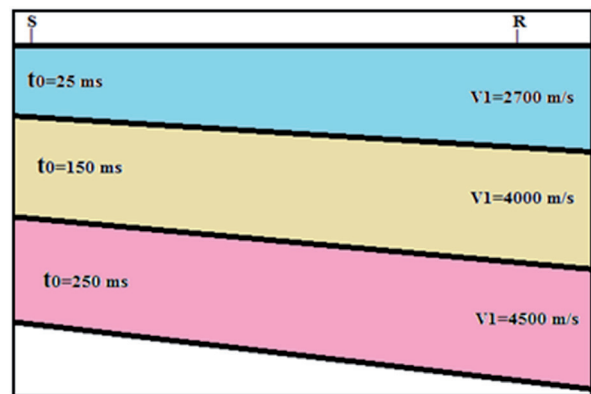

Fig. 3 - Geologic model for generating the synthetic section (S = source and R = receiver).

5. Application to real post-stack seismic section

In the following discussion on the 2DAW filter and AM filter for data filtering, we will assume that the seismic section is a matrix of m rows and n columns with all necessary values outside the seismic section being zero. The proposed filter operates on a α-by-α; α must be an odd value; the single and combined use of 2DAW and AM filters were applied to a stacked portion of a seismic section from the north-western African Sahara. The typical receiver interval is 25 m, the shot interval is 25 m, the field raw stack section consists of nearly 320 traces, the distance between the Common Depth Point (CDP) is 12.5 m, the recording time length is around 1 s, and the data were resampled at 4 ms after processing. The sweep bandwidth has a frequency range of 8-72 Hz and 12 s time length, using a vibrator source. The fold of coverage is 60, each stacked trace is obtained by refraction statics and NMO correction. The raw stacked data is shown in Fig. 5a. Despite the stacking procedure, strong random noise still remains on the stacked section, in addition to poor lateral continuity. The results are compared with the classic and eminent F-K filter.

This seismic section shows strong dipping events and a faulted structure between trace bin number 151 and 225 as indicated by vertical quality degradation. Note the strong noise, which
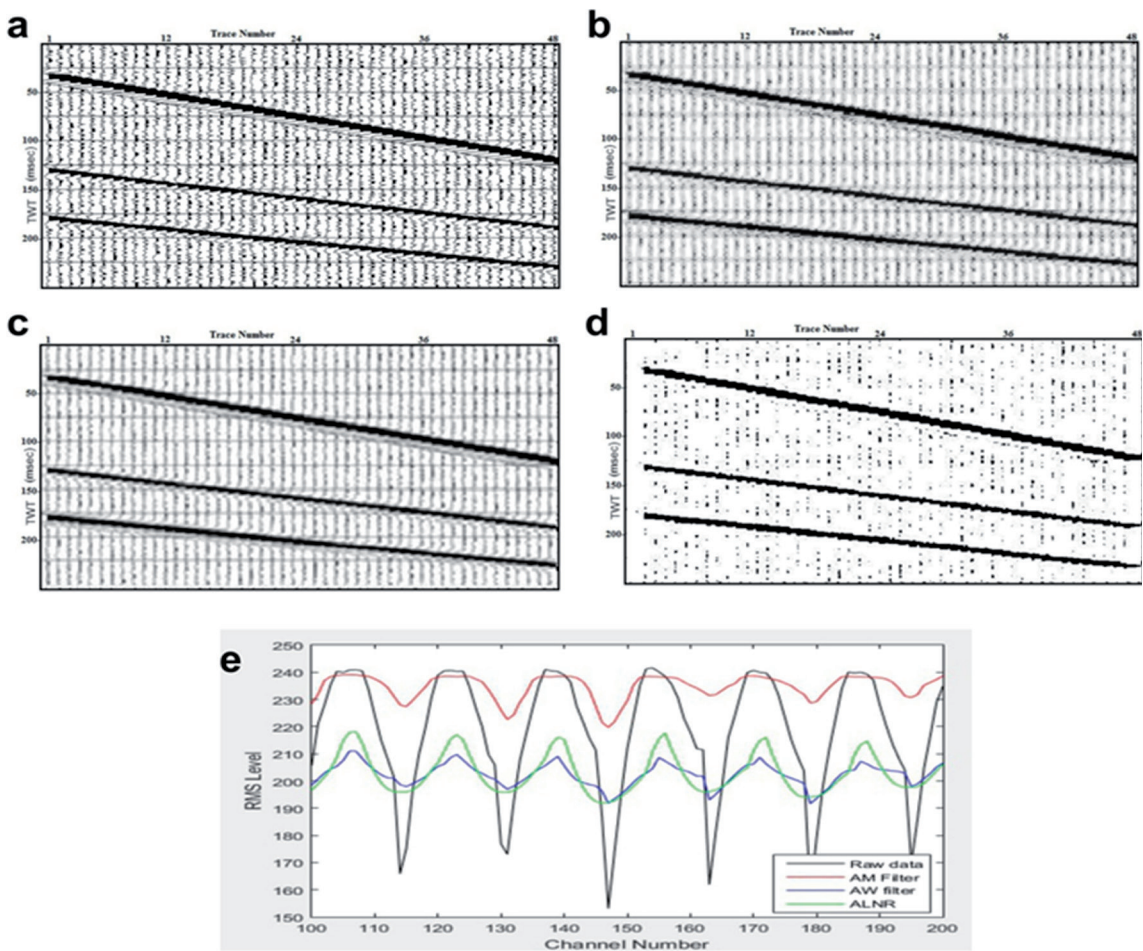
Fig. 4 - Synthetic seismic section; a) original synthetic section by adding 25% of random noise; b) section filtered by 2DAW filter; c) section filtered by ALNR filter; d) section filtered by AM filter; e) comparison graph of RMS level for raw and section obtained by different filters.

masks reflectors and other seismic events, appear in most sections. The adaptive filter is more selective than a comparable linear filter, preserving edges and other high-frequency parts of an image. In this section, we utilise one real field data example to demonstrate the successful performance of the 2DAW filter, AM filter, and ALNR filter.

6. Results and discussion

To demonstrate the successful performance of the used filter, many values of windows (mask) were tested on a seismic image. Some seismic events are attenuated by the F-K filter, where F is the frequency and K refers to wave-number, for example those located between 0.8 to 1.0 s in time and from CDP 50 to 75 and others situated between 0 to 0.6 s in time and from CDP 225 to 301 (Fig. 5b), however, these events are preserved when using adaptive filters. Fig. 5c displays the complete clean seismic section, which contains the clearest events, but some noise that still persists located at 0 to 1 s and from CDP 151 to 225 corresponding to the fault

plane; in this case we have applied the AM filter. In Fig. 5d, the raw stack section is filtered by ALNF using window equal to 9, variance equal to 3, and 3 for threshold value, and it can be seen that random noise is filtered as a whole. With the increase in the order of the window of 2DAW filter, (9×9), as shown in Fig. 5e, the quality of the final document becomes increasingly acceptable. Lastly, we applied the two filters together, the quality in this case of the seismic section is even better and the noise corresponding to the fault plane is better attenuated than before (Fig. 5f).

To quantitatively compare the reconstruction performance, we use the signal-to-noise ratio (SNR) metric defined by the following formula:

$$SNR = 10 \log_{10} \frac{\|d_0\|_2^2}{\|d_0 - d\|_2^2} \tag{9}$$
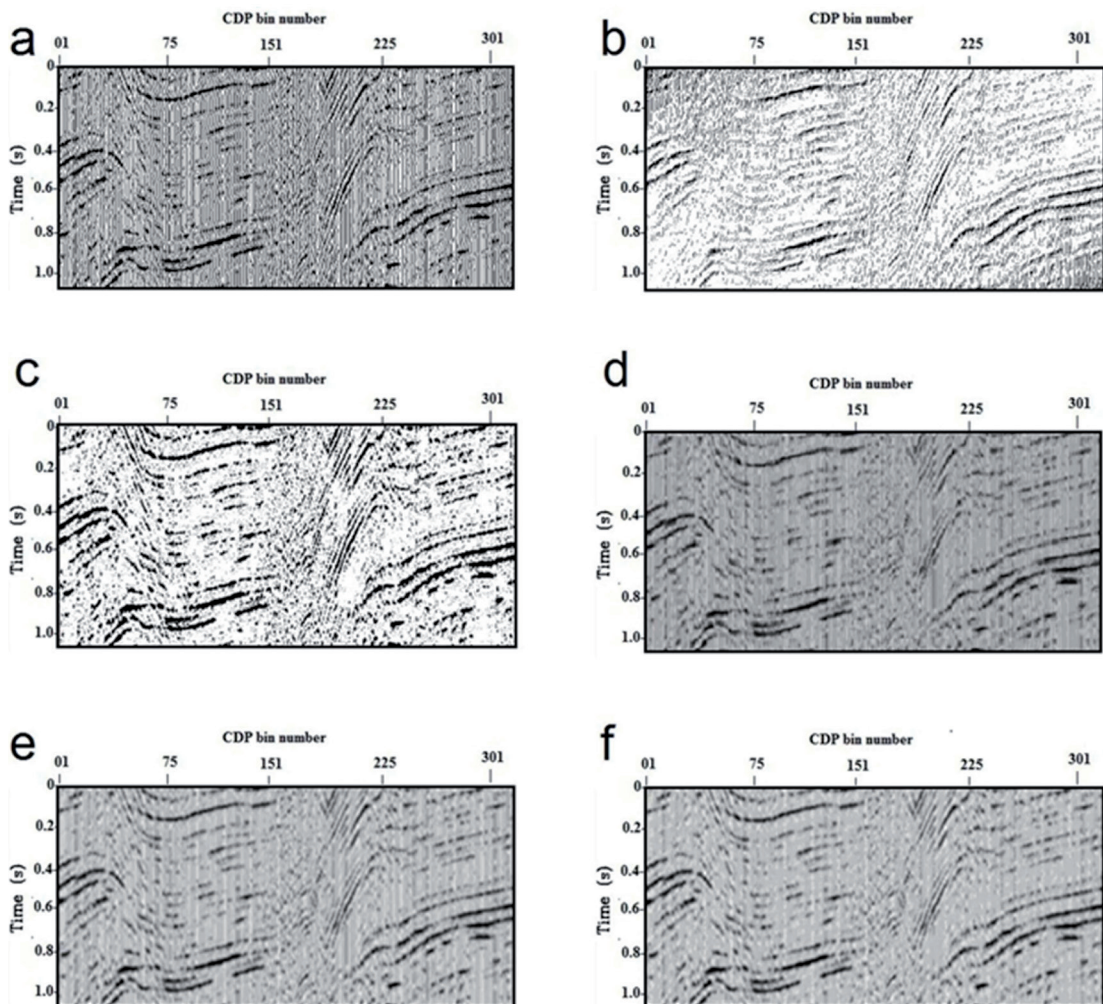

Fig. 5 - Filtered sections: a) raw stack section; b) F-K filter; c) AM filter; d) ALNR filter; e) 2DAW filter with window size of 9×9; f) 2DAW filter with 9×9 window + 2 pass AM filter.

where d_0 is the clean and complete data and d is the noisy or incomplete data (Wu and Bai, 2018). To show the effect of adaptive filters we calculate the SNR for each filter.

The numerical results of the study are presented in Fig. 6a, showing values of SNR for the raw stack processed by different filters. The initial section has a low estimated value (SNR = 1.2842), whereas the ratio is equal to 2.4215 when we use the AM filter and improves to 5.3822 when using the 2DAW filter with a 9×9 window. The best quality is obtained when using both filters such as the AM filter and 2DAW filter (SNR = 5.4735). Also, we note that the use of the ALNR filter alone (Fig. 6b) improves the seismic quality in the same way as in the case when the combined filters are used. It is clear that using various filters and techniques enhances the SNR of the data and concretely improves the seismic image quality.

As the random noise has a random value we can, then, measure the standard deviation of the image. Standard deviation is the most widely used measure of variability or diversity used in statistics. In terms of image processing, it shows how much variation or "dispersion" exists from the average (mean, or expected value) (Longkumer et al., 2014). A high standard deviation indicates that the data points are spread out over a large range of values (Fig. 7e), whereas a low standard deviation indicates that the data points tend to be very close to the mean (Fig. 7f). A simple comparison between the two graphs shows that the standard deviation is reduced to one third, from 120 to 40, after filtering.

6.1. Structural similarity comparison

During the last two decades, the structural similarity index (SSIM) between two images, introduced by Wang et al. (2004), is an efficient tool for assessing image quality and has become an accepted standard among image quality metrics (Dosselman and Yang, 2009). The SSIM formula takes into account luminance, contrast, and structure.
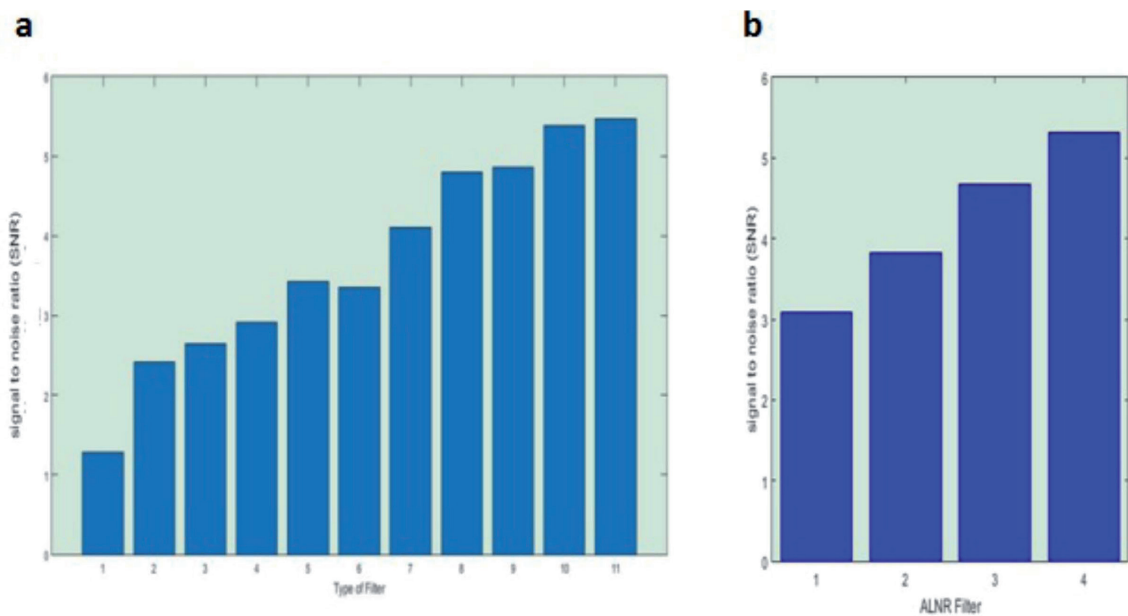

Fig. 6 - Comparison of SNR: a) 1 = raw section, 2 = AM filter, 3 = two pass AM filter, 4 = two pass AM filter + 2DAW 5×5, 5 = two pass AM filter + 2DAW 9×9, 6 = 2DAW 3×3, 7 = 2DAW 5×5, 8 = 2DAW 7×7, 9 = 2DAW 7×7 + 2 AM filter, 10 = 2DAW 9×9, 11 = 2DAW 9×9 + 2 pass AM filter; b): ALNR, 1, 2, 3, and 4, window size of 3, 5, 7, and 9 respectively.

After normalising each image, we have calculated the SSIM and the 2D coefficient correlation between unfiltered and filtered images (Table 1).

Table 1 - SSIM and CORR2 values for each filter.

Filter Type	SSIM	CORR2
2DAW	0.98	0.20
AM	0.99	0.55
ALNR	0.98	0.20
2DAW+AM	0.98	0.32

As shown in Table 1, all values of SSIM are practically the same (0.98 and 0.99) and indicate good structural similarity. The CORR2 measures the correlation coefficient between an image and the same image processed with a different filter; we find that these values are lower than the unit because of the filtering effect that improves image quality.

6.2. Spectral comparison

Discrete Fourier Transform (DFT) is a commonly used and vitally important function for a vast variety of applications. Fourier image analysis simplifies computations by converting complex convolution operations in the spatial domain to simple multiplications in the frequency domain. Due to their computational complexity, DFT often becomes a computational constraint for applications requiring high throughput and near real-time operations. 2D images are, in general, non-periodic, but are assumed to be periodic while calculating their DFT (Mahmood *et al.,* 2015). Fig. 7a shows the spectral magnitude of a raw stack section, whose frequency content is broad, ranging from 200 to 600 in *x* bin number. In Fig. 7b, corresponding to the image filtered by ALNR, the content frequency is different in this case and the spectrum becomes more energetic. Fig. 7c illustrates image spectra for the seismic section when the AM filter was used. We note a certain difference with the one obtained on the original section, this may be interpreted owing to the fact that some noise components have been attenuated by the filtering operation. Finally, the spectrum of the section filtered by the two filters, namely AM filter and 2DAW filter, is shown in Fig 7d. In this case, we can see that the maximum of magnitude spectrum has become more centred and enhanced in the centre and attenuated at the edges.

6.3. Noise comparison

The difference between the unfiltered and filtered image, obviously after normalisation, allows comparing the degree of noise attenuated by each filter (Fig. 8). Fig. 8a represents the noise removed by the 2DAW filter; the rectangle in red shows reflections attenuated by the operation of filtering, the noise attenuated by the AM filter is shown in Fig. 8b, while that attenuated by ALNR and 2DAW + AM filters is shown in Figs. 8c and 8d, respectively. As we know the purpose of filtering is to attenuate the noise without damaging the signal, and it can be seen that in the case of the ALNR filter, the attenuation of reflections is relatively low. The power of noise is also calculated for each filtering operation (Figs. 8e and 8f): we can see that the noise attenuated by ALNR is important in power (represented in blue colour).
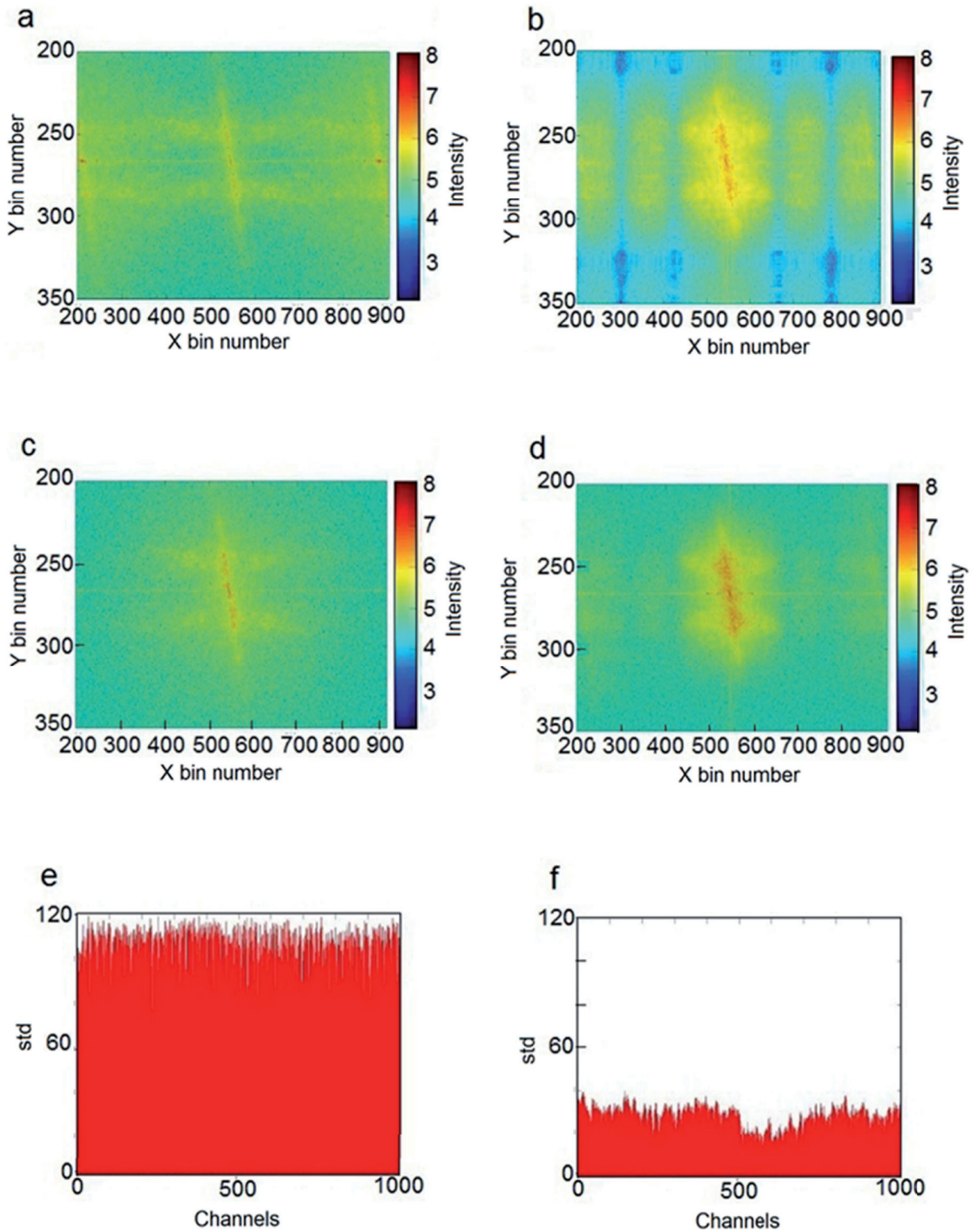
Fig. 7 - 2D spectrum of sections: a) raw stack; b) ALNR filter; c) AM filter; d) 2DAW 9×9 window size + 2 pass AM filter, and standard deviation for: e) raw stack; f) 2DAW 9×9 + 2 pass AM filter.
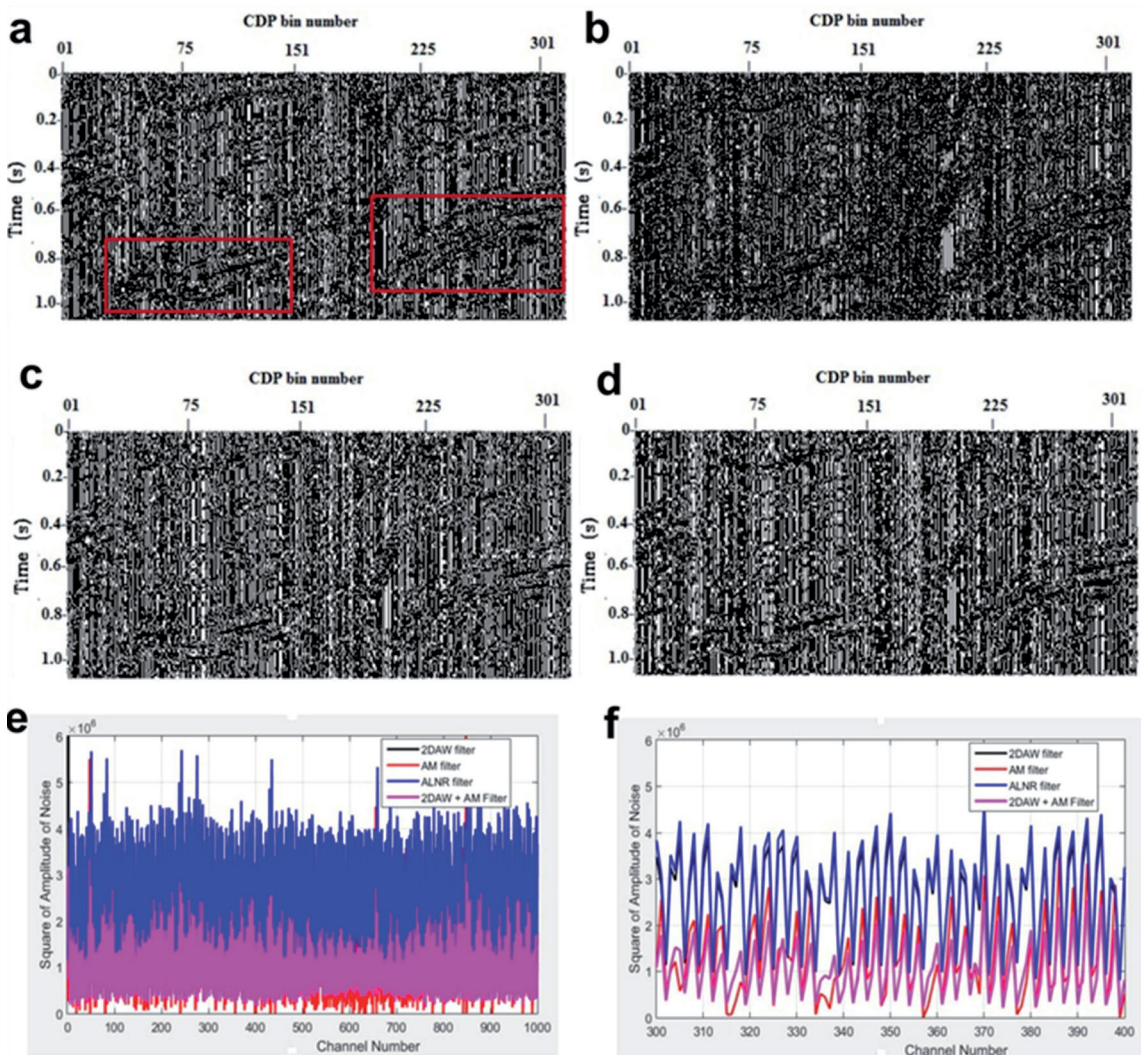
Fig. 8 - Difference between raw seismic image and filtered seismic image: a) 2DAW filter; b) AM filter; c) ALNR filter; d) 2DAW + AM filter; e) the power of noise for each residual image; f) zoom of Fig. 8e between 300 and 400 channel number.

7. Conclusion

Through this study we were able to explore two kinds of filters, separately and combined, namely the 2DAW and AM filters, and new application of the ALNR filter on a seismic image in order to reduce random noise. The results are compared with the classic and eminent F-K filter: the proposed filters have an obvious advantage over the conventional filter. By comparing different filtered seismic sections and their spectra, it is recommended to use combined adaptive Wiener and AM filters. We also noted no blurring in the image when using the ALNR filter, which has an advantage over the Wiener filter. The validation of such filters was carried out on synthetic and real stacked seismic sections. Nevertheless, the quality of the filtered image remains dependent on the good choice of filter parameters, as well as the size of the window.

REFERENCES

Bai M. and Wu J.; 2017: *Efficient deblending using median filtering without correct normal moveout-with comparison to migrated images*. J. Seismic Explor., 26, 455-476.

Bankman H.I.; 2009: *Handbook of medical image processing and analysis*. 2nd ed. Elsevier Inc., Amsterdam, the Netherlands, 970 pp.

Bekara M. and Baan M.V; 2009: *Random and coherent noise attenuation by empirical mode decomposition*. Geophys., 74, 89-98.

Bednar J.B.; 1983: *Applications of median filtering to deconvolution, pulse estimation, and statistical editing of seismic data*. Geophys., 48, 1598-1610, doi: 10.1190/1.1441442.

Cai H-P., He Z-H., Li Y-L., He G-M., Zou W., Zhang D-J. and Liu P.; 2014: *An adaptive noise attenuation method for edge and amplitude preservation*. Appl. Geophys., 11, 289-300, doi: 10.1007/s11770-014-0446-0.

Canales L.L.; 1984: *Random noise reduction.* In: Expanded Abstracts, 54th Annual Meeting, SEG Technical Program, Atlanta, GA, USA, pp. 525-527, doi: 10.1190/1.1894168.

Chen Y. and Ma J.; 2014: *Random noise attenuation by f-x empirical mode decomposition predictive filtering*. Geophys., 79, 81-91.

Chen Y., Zu S., Wang Y. and Chen X.; 2020: *Deblending of simultaneous source data using a structure-oriented space-varying median filter*. Geophys. J. Int., 222, 1805-1823, doi: 10.1093/gji/ggaa189.

Chotikawanid P., Pramoun T., Thongkor K., Supasirisun P. and Amornraksa T.; 2018*: Image watermarking using adaptive local noise reduction filter*. In: Proc., 15th International Conference on Electrical Engineering/ Electronics, Computer, Telecommunications and Information Technology (ECTI-CON), Chiang Rai, Thailand, pp. 154-157, doi: 10.1109/ECTICon.2018.8619993.

Deng X., Haitao M., Yue L. and Qian Z.; 2015: *Seismic random noise attenuation based on adaptive time-frequency peak filtering*. J. Appl. Geophys., 113, 31-37.

Dosselman R. and Yang X.D.; 2009: *A comprehensive assessment of the structural similarity index*. Signal Image Video Process*., 5, 81-91, doi: 10.1007/s11760-009-0144-1.

Dragoset B.; 1995: *Geophysical applications of adaptive noise cancellation*. In: Expanded Abstracts, 27th Annual OTC, SEG Technical Program, Houston, TX, USA, pp. 1389-1392, doi: 10.4043/7655-MS, doi: 10.1190/1.1887226.

Gan S., Wang S., Chen Y., Chen X. and Xiang K.; 2016: *Separation of simultaneous sources using a structural-oriented median filter in the flattened dimension*. Comput. Geosci., 86, 46-54, doi: 10.1016/j.cageo.2015.10.001.

Gonzales R.C and Woods R.E.; 2002: *Digital image processing, 2nd ed*. Prentice-Hall, Upper Saddle River, NJ, USA, 807 pp.

Jeng Y., Li Y-W., Chen C-S. and Chien H-Y.; 2009: *Adaptive filtering of random noise in near-surface seismic and ground-penetrating radar data.* J. Appl. Geophys., 68, 36-46.

Jiang X. and Mojon D.; 2003: *Adaptive local thresholding by verification-based multithreshold probing with application to vessel detection in retinal images*. IEEE Trans. Pattern Anal. Mach. Intell., 25, 131-137.

Lee J.S.; 1980: *Digital image enhancement and noise filtering by use of local statistics*. IEEE Trans. Pattern Anal. Mach. Intell., 2, 165-168.

Liu C., Liu Y., Wang D. and Sun J.; 2006: *A 2D multistage median filter to reduce random seismic noise*. Geophys., 71, V105-V110, doi: 10.1190/1.2236003.

Liu J., Hu B. and Wang Y.; 2019: *Optimum adaptive array stochastic resonance in noisy grayscale image restoration*. Phys. Lett. A, 383, 1457-1465, doi: 10.1016/j.physleta.2019.02.006.

Longkumer N., Kumar M., Jaiswal A.K. and Saxena R.; 2014: *Contrast enhancement using various statistical operation and neigbourhood processing*. Signal Image Process. Int. J. (SIPIJ), 5, 51-61, doi: 10.5121/ sipij.2014.5205.

Mahmood F., Toots M., Öfverstedt L-G. and Skoglund U.; 2015: *2D discrete Fourier transform with simultaneous edge artifact removal for real-time applications*. In: Proc., International Conference on Field Programmable Technology (FTP), Queenstown, New Zealand, pp. 236-239, doi: 10.1109/FPT.2015.7393157.

Mohamed K. and Hardie R.C.; 2015: *A collaborative adaptive Wiener filter for image restoration using a spatial-domain multi-patch correlation model*. J. Adv. Signal Process., 6, 23 pp., doi: 10.1186/s13634-014-0189-3.

Neelamani R., Baumstein A.I., Gillard D.G., Hadidi M.T. and Soroka W.L.; 2008: *Coherent and random noise attenuation using the curvelet transform*. The Leading Edge, 27, 240-248.

Rajesh R., Tiwari R.K., Dhanam K. and Seshunarayana T.; 2014: *T-x frequency filtering of high resolution seismic reflection data using singular spectral analysis*. J. Appl. Geophys., 105, 180-184, doi: 10.1016/j.jappgeo.2014.03.017.

Rakesh M.R.; 2018: *Novel algorithm of adaptive median filter for removal of noises in both image and signal processing*. Int. J. Adv. Res. Electr. Electron. Instrum. Eng., 7, 2801-2806, doi: 10.15662/IJAREEIE.2018.0706002.

Ristau J.P. and Moon W.M; 2001: *Adaptive filtering of random noise in 2-D geophysical data*. Geophys., 66, 342-349.

Saad O. and Chen Y.; 2020: *Deep denoising autoencoder for seismic random noise attenuation*. Geophys., 85, 367-376, doi: 10.1190/GEO2019-0468.1.

Sacchi M. and Naghizadeh M.; 2009: *Adaptive linear prediction filtering for random noise attenuation*. In: Proc., SEG International Exposition and Annual Meeting, Houston, TX, USA, 3347-3351, doi: 10.1190/1.3255555.

Sayed A.H.; 2003: *Fundamentals of adaptive filtering.* John Wiley & Sons, Hoboken, NJ, USA, 1168 pp.

Shang S., Han L-G., Lv Q-T. and Tan C-Q.; 2013: *Seismic random noise suppression using an adaptive nonlocal means algorithm*. Appl. Geophys., 10, 33-40, doi: 10.1007/s11770-013-0362-8.

Stewart R.R. and Schieck D.G.; 1993: *3-D fk filtering*. J. Seismic Explor., 2, 41-54.

Telford W.M., Geldart L.P. and Sheriff R.E.; 1990: *Applied geophysics*. Cambridge University Press, Cambridge, UK, 770 pp., doi: 10.1017/CBO9781139167932.

Wang Z., Sheikh H.R., Bovik A.C and Simoncelli E.P.; 2004: *Image quality assessment: from error visibility to structural similarity*. IEEE Trans. Image Process., 13, 600-612, doi: 10.1109/TIP.2003.819861.

Westin C-F., Knutsson H. and Kikinis R.; 2000: *Adaptive image filtering.* In: Handbook of Medical Imaging, Bankman I.N. (ed), Academic Press, San Diego, CA, USA, pp. 19-32.

Widrow B.; 1959: *Adaptive sampled-data systems - A statistical theory of adaptation*. IRE WESCON Convention Record, 4, 74-85, <isl.stanford.edu/~widrow/papers/c1959adaptivesampled.pdf>.

Wu J. and Bai M.; 2018: *Adaptive rank-reduction method for seismic data reconstruction*. J. Geophys. Eng., 15, 1688-1705, doi: 10.1093/jge/aabc74.

Yilmaz Ö.; 2001: *Seismic data analysis: processing, inversion, and interpretation of seismic data*. Investigation in Geophysics, Society of Exploration Geophysics Book, Tulsa, Ok, USA, 2027 pp.

Zhenghao S. and Ko B.F.; 1994: *A comparison of digital Speckle filters.* In: Proc., IEEE International Geoscience and Remote Sensing Symposium, Pasadena, CA, USA, pp. 2129-2133, doi: 10.1109/IGARSS.1994.399041.

Corresponding author: Lakhdar Harrouchi
                           Sahara Geology Laboratory, Kasdi Merbah University
                           P.O. Box 511, Ouargla 30000, Algeria
                           Phone: +213 66 6323288; e-mail: Harrouchi_lakhdar@yahoo.fr